Modeling the sorption dynamics of NaH using a reactive force field

J. G. O. Ojwang,[1,a)] Rutger van Santen,[1] Gert Jan Kramer,[1] Adri C. T. van Duin,[2] and William A. Goddard III[2]
[1]*Schuit Institute of Catalysis, Eindhoven University of Technology, Postbus 513, 5600 MB, Den Dolech 2, Eindhoven, The Netherlands*
[2]*Material Research Center, California Institute of Technology(Caltech), 1200 East California Boulevard, Pasadena, California 91125, USA*

(Received 12 December 2007; accepted 17 March 2008; published online 28 April 2008)

We have parametrized a reactive force field for NaH, $ReaxFF_{NaH}$, against a training set of *ab initio* derived data. To ascertain that $ReaxFF_{NaH}$ is properly parametrized, a comparison between *ab initio* heats of formation of small representative NaH clusters with $ReaxFF_{NaH}$ was done. The results and trend of $ReaxFF_{NaH}$ are found to be consistent with *ab initio* values. Further validation includes comparing the equations of state of condensed phases of Na and NaH as calculated from *ab initio* and $ReaxFF_{NaH}$. There is a good match between the two results, showing that $ReaxFF_{NaH}$ is correctly parametrized by the *ab initio* training set. $ReaxFF_{NaH}$ has been used to study the dynamics of hydrogen desorption in NaH particles. We find that $ReaxFF_{NaH}$ properly describes the surface molecular hydrogen charge transfer during the abstraction process. Results on heat of desorption versus cluster size shows that there is a strong dependence on the heat of desorption on the particle size, which implies that nanostructuring enhances desorption process. To gain more insight into the structural transformations of NaH during thermal decomposition, we performed a heating run in a molecular dynamics simulation. These runs exhibit a series of drops in potential energy, associated with cluster fragmentation and desorption of molecular hydrogen. This is consistent with experimental evidence that NaH dissociates at its melting point into smaller fragments. © *2008 American Institute of Physics*. [DOI: 10.1063/1.2908737]

I. INTRODUCTION

Parametrization of a reactive force field ($ReaxFF_{NaH}$) for sodium and sodium hydride has been done with the objective of describing the H_2 desorption process in NaH. ReaxFF has already been shown to be able to accurately predict the dynamical and reactive processes in hydrocarbons,[1] silicon/silicon oxides,[2] aluminum/aluminum oxides,[3] and nitramines.[4] In this work, details of the parametrizations of $ReaxFF_{NaH}$, diffusion mechanism of hydrogen atoms and hydrogen molecules in NaH, and abstraction process of surface molecular H_2 in NaH cluster are examined. The details on the parametrizations procedure coupled with tests conducted to ensure that the force field is properly parametrized as per the *ab initio* derived data inputs are discussed. The parametrized force field, $ReaxFF_{NaH}$, has been used to study the dynamical details of abstraction of molecular hydrogen from NaH cluster. A molecular dynamics simulation on $Na_{48}H_{48}$ cluster has been done and it is found that the fall in potential energy is associated with either cluster fragmentation or desorption of molecular hydrogen. Modeling of $ReaxFF_{NaH}$ is a first step toward our goal of parametrizing a reactive force field ($ReaxFF_{NaAlH_4}$) to study the structural and dynamical details of hydrogen ab(de)sorption processes in $NaAlH_4$ system. We aim to elucidate on the long range transport mechanisms of Al atoms during ab(de)sorption process and the dynamics governing hydrogen desorption coupled with getting a better insight on the exact role of titanium during the decomposition process of $NaAlH_4$.

In crystalline form, NaH adopts a NaCl-type structure in which each Na^+ ion is surrounded by six H^+ ions in an octahedral configuration. At elevated temperatures of 698 K,[5] NaH undergoes thermal decomposition in which molecular hydrogen is released. This release temperature is lower than the melting point of NaH, 1073 K, but is much higher than the melting point of sodium, 371 K. Theoretically, Ke and Tanaka found that the desorption of hydrogen takes place at 726 K.[5] The thermal desorption process of molecular hydrogen from NaH proceeds as follows:

$$\mathrm{NaH} \rightarrow \mathrm{Na} + \tfrac{1}{2}\mathrm{H}_2. \quad (1)$$

This paper is organized as follows. The first part deals with force field parametrizations, the second part focuses on the tests taken to ensure that the force field is well parametrized, and the last part deals with molecular dynamics simulation using the parametrized force field.

II. FORCE FIELD PARAMETRIZATION

Parametrization of $ReaxFF_{NaH}$ has been done in line with the methodology used to develop $ReaxFF_{MgH}$.[6] A key feature in ReaxFF is using the bond-order formalism that allows for bond breaking and formation as per Tersoff,[7] Brenner,[8] and environment dependent interatomic potential[9] approach. ReaxFF includes polarizable charges calculated using electronegativity equalization method (EEM),[10] which provides a ge-

[a)]Electronic mail: j.g.o.ojwang@tue.nl.

TABLE I. Bond energy and bond order parameters. D_e^σ is in kcal/mol.

Bond	D_e^σ	$P_{be,1}$	$P_{be,2}$	$P_{b0,1}$	$P_{b0,2}$
Na–Na	60.0	−0.3548	2.4578	−0.05	4.518
Na–H	87.7	−0.7276	1.1502	−0.20	4.818

ometry dependent charge distribution. ReaxFF calculates nonbonded (van der Waals and Coulomb) interactions between all atoms (including 1-2, 1-3, and 1-4 interactions).

The quantum mechanical data used in fitting ReaxFF parameters were obtained from VASP,[11] using a projector augmented[12] plane-wave method. The Kohn–Sham ground state is self-consistently determined in an iteration matrix diagonalization scheme of band by band. The exchange correlation effects for a particular ionic configuration is described by the generalized gradient approximation of Perdew and Wang.[13–15] For the NaH phases, Brillouin zone integrations were performed using $13\times13\times13$ *k*-points as per the Monkhorst–Pack (MP) grid procedure,[16] whereas for sodium the following *k*-points were used: Na-fcc$(11\times11\times11)$, Na-bcc$(11\times11\times11)$, Na-hcp$(11\times11\times11)$, and Na-sc$(17\times17\times17)$. With these *k*-points, a total-energy convergence of within 1 meV was achieved. The reference configurations for valence electrons used were Na$(3s^1)$ and H$(1s^1)$. For all volumes of the structures considered, the structures were fully optimized using force as well as stress minimization. The ions involved are steadily relaxed toward equilibrium until the Hellman–Feynman forces are minimized to less than 0.01 meV/Å, using a conjugate gradient algorithm during all relaxation runs. In all calculations, a well converged plane-wave cutoff of 600 eV was used. To determine the equations of state (EOS), for a fixed cell volume of each structure, the cell shape and atomic coordinates were fully optimized until the forces were less that 1 meV eV/Å per atom. The structure with the lowest energy was then determined by plotting a total energy versus cell-volume curves for all the structures considered and then fitted to a Birch–Murnaghan EOS.[17]

Since VASP is a plane-wave code, it cannot compute Mulliken populations analysis. Mulliken population analysis is implemented in CRYSTAL06,[18] which uses a periodic localized basis set approach. Therefore, to determine the partial charges of the atoms in the crystal, the cell parameters of the optimized structure in VASP were used as input in single point calculations in CRYSTAL06. Mulliken population analysis was then performed on the atoms in the crystal to obtain the Mulliken charges. In CRYSTAL06, an all electron calculation was performed. The radical factors in the all electron basis set are expressed as a linear combination of Gaussian type Functions of the electron-nucleus distance according to 8(s)511(sp)G and 5(s)11(sp)1(p)G contractions for Na and H, respectively.[19] To ensure high numerical accuracy, the truncation tolerance for the numerical evaluation of bielectronic integrals (both the Coulomb and the HF exchange series) were set at 10^{-8}, 10^{-8}, 10^{-8}, 10^{-8}, and 10^{-16}.[19] All the units are in a.u. Sampling points for Brillouin zone integration were generated using the MP scheme.[16] We used 14 *k*-points in the irreducible Brillouin zone. The Gilat net[20] was also set at 14 *k*-points. The convergence criteria on the total energy was set at 10^{-7} a.u.

Parametrization of the ReaxFF energy expressions was done by fitting to a training set containing the density functional theory (DFT) derived EOSs of pure Na and NaH condensed phases, reaction energies, and bond dissociation profiles on small finite clusters. Phase transformations/crystal modifications in both Na and NaH systems during desorption process was accounted for by adding the high pressure phases of Na and NaH in addition to the ground state phase to the quantum mechanical calculations. In the case of Na, we considered four phases: bcc-Na(8-coordinate), sc-Na(6-coordinate), fcc-Na(12-coordinate), and hcp-Na(12-coordinate). For NaH, the high pressure (CsCl-type) and NaCl-type phases were considered.

The bond and atom parameters for the ReaxFF energy functions (Tables I and II) were determined from Na–Na and Na–H bonds in small NaH clusters such as NaH, Na_2H_2, Na_3H_3, and Na_4H_4 and from the EOS and cohesive energies of Na metal and NaH condensed phases. The symbols of the parameters in Tables I–IV are shown in Refs. 2 and 4.

The EEM parameters (EEM hardness η, EEM electronegativity χ, and EEM-shielding parameter γ), which were parametrized to fit Mulliken charge distributions of small representative structures (NaH, Na_2H_2, Na_3H_3, and Na_4H_4) obtained from DFT calculations are shown in Table III. ReaxFF successfully reproduces charge transfer for all the clusters considered.

For the valence angle parameters, two case have been considered: H–Na–Na and H–Na–H. The clusters are first fully optimized in DFT calculations. This is followed by doing single point calculations in which the valence angles are modified while other parameters are fixed. Table IV shows the optimized valence angle parameters. The first line reflects a normal H–Na–Na angle interaction with an equilibrium angle of 131.67° and force constants of 2.0048 and 5.0 kcal. The second line aims to destabilize the Na–H–Na configura-

TABLE II. Atom parameters.

Atom	$p_{ov/un}$	λ_{11}	$p_{v,5}$	$p_{v,6}$
Na	−2.50	3.99	8.0	2.5791
H	−15.76	2.15	1.0	2.8793

TABLE III. Coulomb parameters.

Atom	η(eV)	χ(eV)	γ(Å)
Na	5.0	−0.3531	0.3669
H	6.5	4.1882	0.7358

TABLE IV. Valence angle parameters.

Angle	$\Theta\Theta^{\circ}_{0,0}$	k_a	k_b	$p_{v,1}$	$p_{v,2}$	p_{pen}	$p_{v,4}$
H–Na–Na	131.67	2.0048	5.0	0	0.7765	0	1.76
H–Na–Na	180.00	−27.9700	29.33	0	1.0074	0	1.56

tion (with the H directly in between the Na atoms). Without the second angle, this configuration gets to be too stable.

A. Bond dissociation and binding energies

The bond energy in the reactive potential was optimized using DFT derived values of bond dissociation profiles of small NaH clusters. Figure 1 shows the bond dissociation curve of NaH. The dissociation curves were constructed from the equilibrium geometry through single point calculations by changing the bond length. For the DFT case, both the singlet and triplet states were considered. ReaxFF gives an equilibrium bond length of 1.91 Å, whereas DFT gives a value of 1.895 Å. Chen *et al.*[21] computed a theoretical Na–H bond length of 1.913 Å at the QCISD/6-311G** level of theory.[21]

Another key test is on the adsorption energies on the Na surfaces. For (100) hollow site, DFT gives a value of 5.4 kcal/mol H_2, while ReaxFF gives 10.4 kcal/mol H_2 (see Fig. 2). For (100) bridge site, DFT predicts the adsorption energy to be 3.1 kcal/mol H_2, while ReaxFF predicts −1.7 kcal/mol H_2. For the (100) top site DFT gives an adsorption energy of 57.4 kcal/mol H_2, while ReaxFF predicts 49.5 kcal/mol H_2.

B. Heats of formation

The possibility of a large cluster of NaH fragmenting into smaller clusters during heating runs was also considered by fitting into the training set the heats of formation of NaH, Na_2H_2, Na_3H_3, and Na_4H_4 clusters. The results are shown in Table V. The DFT's endothermic heat of formation of gas-phase NaH from atomic Na and molecular hydrogen is 28.51 kcal/mol, which is in good agreement with the literature value of 29.7 kcal/mol.[22] ReaxFF, on the other hand, gives a value of 6.91 kcal/mol. The table shows that there is

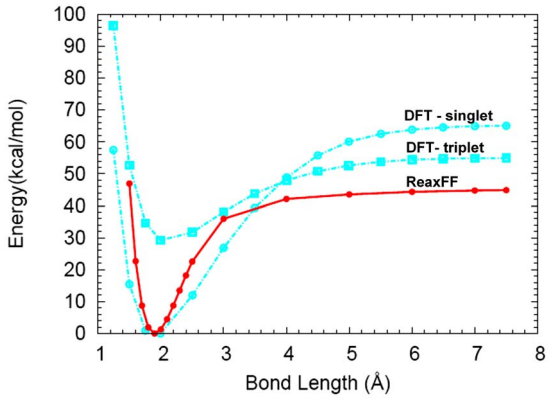

FIG. 1. (Color online) Bond dissociation curves of small clusters of NaH as calculated by DFT and ReaxFF. The energies were computed with reference to the equilibrium bond length's energy. In the case of DFT, the equilibrium energy of the singlet state was used as a reference.

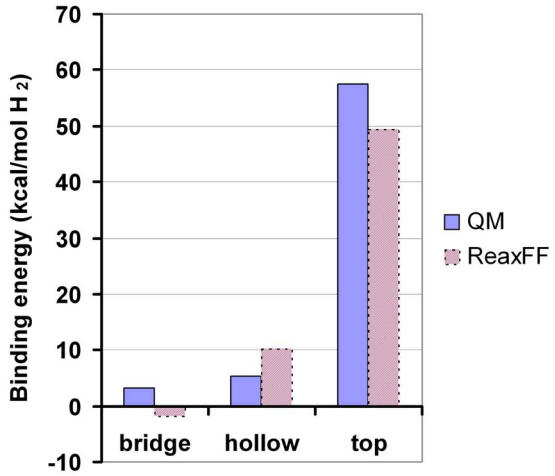

FIG. 2. (Color online) Binding energies of dissociated H_2 on high symmetry sites on Na (100) surface.

good agreement on the heats of formation between ReaxFF and DFT with increasing cluster size. For Na_4H_4, DFT gives a value of −8.53 kcal/mol for the heat of formation, whereas ReaxFF gives a value of −6.92 kcal/mol. This mismatch between DFT and ReaxFF values on the heat of formation a single NaH molecule is an artifact of ReaxFF. As the size of the cluster increases, the values of ReaxFF closely parallels DFT values. For instance, for Na_3H_3 the heats of formation are −6.3 and −5.1 kcal/mol as computed by DFT and ReaxFF, respectively. The increase in heat of formation with cluster size indicates the importance of ionicity (electrostatics) on chemical bonding in these systems.

For the condensed phase, the experimental heat of formation of NaH is −13.49 kcal/mol.[23] DFT gives a heat of formation value of −10.19 kcal/mol, while ReaxFF gives −11.60 kcal/mol. Table VI shows the interatomic distances and angles within the clusters calculated by DFT, ReaxFF, and from Ref. 21. For the atomic distances, the ReaxFF values are consistent with the DFT values. For instance, from the DFT computation, the Na–H distance in NaH cluster is 1.895 Å, whereas ReaxFF gives 1.908 Å. For Na_4H_4 cluster, DFT gives a Na–H distance of 2.048 Å, whereas ReaxFF gives 2.059 Å. For the angles, ReaxFF approximates DFT values as the size of the cluster increases. For instance, from the DFT calculation, the Na–H–Na angle in Na_2H_2 is 82.27°, whereas ReaxFF gives a value of 107.58°, a difference of 25.31°. In Na_3H_3, DFT computes the Na–H–Na to be 109.58°, whereas ReaxFF gives 124.35°, a difference of 14.37°. In Na_4H_4, DFT gives Na–H–Na angle of 130.64°, whereas ReaxFF gives 131.86°, a difference of 1.22°. Thus, as the size of the cluster increases, ReaxFF gives values that

TABLE V. Heat of formation, ΔH_f (in kcal/mol-NaH) of small NaH clusters used in the training set.

Cluster	DFT	ReaxFF
NaH	28.5	6.9
Na_2H_2	0.8	−1.6
Na_3H_3	−6.3	−5.1
Na_4H_4	−8.5	−6.9

TABLE VI. DFT and ReaxFF bond distances and bond angles of small NaH clusters. ReaxFF values are bracketed in bold while the values in square brackets are from Ref. 21, which were computed at the MP2/6–311++G** level of theory.

Cluster	Distance (Å) d_{Na-H}	Angle (deg) Na–H–Na	Angle (deg) H–Na–H
NaH	1.895(1.91)[1.908]		
Na_2H_2	2.106(2.075)[2.121]	82.27(107.58)[84]	97.73(72.43)[96]
Na_3H_3	2.062(2.074)[2.079]	109.98(124.35)[112]	129.96(115.68)[128]
Na_4H_4	2.048(2.069)[2.059]	130.64(131.86)[127]	144.94(138.30)[144]

closely parallel the DFT values. This is the reason why the values of heat of formation of NaH clusters as computed by ReaxFF tend toward DFT values with increase in cluster size. It is worth noting that this artifact of ReaxFF is not a problem because the larger clusters are more relevant during the thermal decomposition of NaH. The smaller cluster, being very unstable, is less likely to appear during the dissociation of larger clusters of NaH.

C. Structural properties

The structural properties of NaH in the NaCl phase were computed by doing a fit to the total energy versus cell-volume data, as calculated by DFT and ReaxFF using the Birch–Murnaghan EOS.[17] The structural properties of NaH NaCl-type calculated using DFT and ReaxFF are given in Table VII.

DFT gives a bulk modulus value of 23.7 GPa, whereas ReaxFF gives 29.2 GPa. These values are consistent with the experimental bulk modulus of 19.4 ± 2.0 GPa (Ref. 24) and theoretical values of 22.8 GPa (Ref. 25) and 27 GPa.[26] For the NaCl-type phase, the equilibrium lattice constant as computed by DFT is 4.8215 Å, while ReaxFF gives lattice constant of 4.775 Å. The experimental value of lattice constant is 4.91 Å (at 298 K).[24] For the CsCl-type phase, ReaxFF gives an equilibrium lattice constant of 2.993 Å which agrees well with the DFT value of 2.995 Å.

For both Na and NaH, the ability of ReaxFF to capture the relative stability of their condensed phases was tested against a number of Na and NaH crystal modifications. For each phase of Na metal (fcc, hcp, sc, and bcc) and NaH (NaCl and CsCl types) considered in this work, the quantum energies were computed for a broad range of volumes, describing both expansion and compression. Figures 3 and 4 compare the ReaxFF results against the DFT values. ReaxFF correctly describes the EOS for NaH phases and excellently estimates the relative phase stability of the two phases vis-à-vis the DFT predictions. DFT predicts that NaCl-type is 7.24 kcal/mol more stable than the CsCl-type phase, while ReaxFF gives a value of 5.83 kcal/mol.

TABLE VII. Equilibrium lattice constant a_0 (Å), bulk modulus B_0 (GPa) and the pressure derivative of the bulk modulus B_0' for NaH on NaCl-type phase calculated using DFT and ReaxFF. Experimental values and theoretical calculations from other workers are also shown.

	a_0	B_0	B_0'	Temp
DFT (this work)	4.82	23.7	3.8	0
ReaxFF	4.77	29.2		0
Expt. (298 K)	4.91[a]	19.4 ± 0.2[a]	4.4 ± 0.5[a]	298
Theor	4.77[b]	27[b]	3.7[b]	0
	4.92[b]	20[b]	4.1[b]	0[c]
	4.89[d]	23.4[d]		0[c]
	4.74(4.87)[e]	27.2(24)[e]		0

[a]Reference 24.
[b]Reference 26.
[c]Zero point energy included.
[d]Reference 5.
[e]Reference 30.

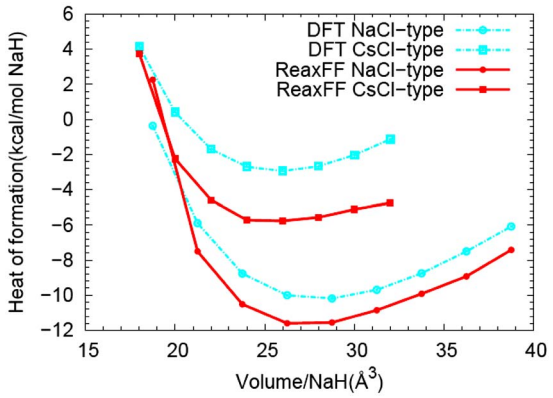

FIG. 3. (Color online) Equations of state for two phases(NaCl-type and CsCl-type) of NaH as computed from DFT and ReaxFF.

In Fig. 4(a), we see that ReaxFF correctly describes the relative phase stabilities of three phases of sodium metal although ReaxFF gives a rather flat curve for the volume expansion parts of the EOS. However, this will not cause a problem since the most relevant and physically interesting parts are the equilibrium volumes from which the relative phase stabilities are deduced. Moreover, all the metal phases dissociate smoothly to give the right dissociation energy [ReaxFF gives 21.61 kcal/mol for the atomization of bcc-Na-metal, experiment gives 25.90 kcal/mol (at 25°)[27] and DFT gives 28.5 kcal/mol]. Figure 4(b) shows that ReaxFF produces the right dissociation curve at higher volumes for the bcc phase. The energies in Fig. 4 are computed with respect to the bcc structure's equilibrium volume energy. DFT predicts that the bcc phase is more stable than the fcc, A15, and sc phases by 0.34, 0.64, and 3.76 kcal/mol, respectively. ReaxFF, on the other hand, predicts that the bcc phase is more stable than the fcc, A15, and sc phases by 0.32, 0.54, and 1.65 kcal/mol, respectively.

III. ABSTRACTION OF HYDROGEN

In order to get a better insight of crystal transformation during the desorption of hydrogen, we simulated successive abstraction of surface molecular hydrogen from $Na_{48}H_{48}$ cluster (see Fig. 5). The abstraction process is given by

$$Na_{48}H_{n+2} \rightarrow Na_{48}H_n + H_2, \quad (2)$$

where $n=46-0$. In the abstraction process, clusters were minimized to find the nearest metastable conformation and then equilibrated at 300 K for 50 000 steps (using a time step of 0.25 fs). The clusters were then annealed to 0 K, after

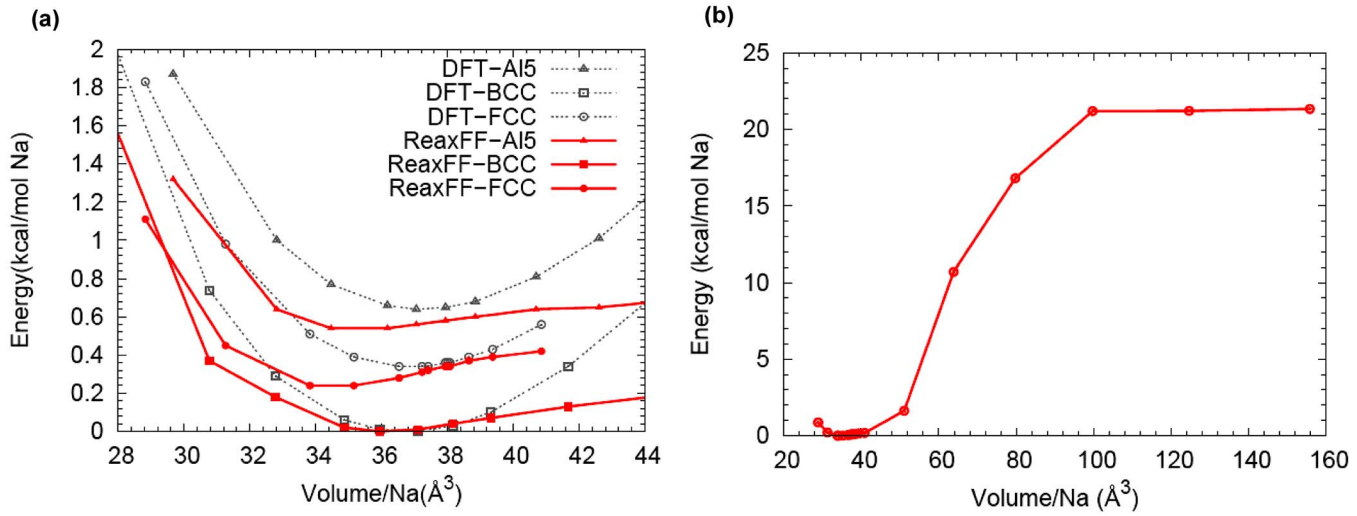

FIG. 4. (Color online) (a) Equations of state (compression and expansion) for three crystal structures (Al5, bcc, and fcc) of Na phases as computed by DFT and ReaxFF. (b) Equation of state of the bcc phase including volume expansions to the dissociation limit. In both cases, the energies are calculated with respect to the equilibrium energy of the bcc phase.

which H_2 abstraction was simulated by removing two hydrogen atoms from the 0 K configuration. This was done iteratively until all the H_2 atoms were removed.

There are two stages shown in Fig. 6(a), which shows that there is a nonlinear trend in particle stability with respect to molecular hydrogen abstraction. During the abstraction process, the surface hydrogen atoms are removed first since they have less number of neighbor and therefore lower stability. Upon hydrogen depletion, some of the bulk Na atoms comes to the surface to replace the depleted hydrogen atoms. In the initial structure, the surface hydrogen atoms mostly occupy the less stable twofold (bridge) sites. However, as more and more surface molecular hydrogen are abstracted, the remaining hydrogen atoms adopt a subsurface conformation and they occupy threefold and fourfold sites. With increasing depletion of hydrogen atoms, the sodium atoms in the bulk replace the depleted hydrogen atoms. These remaining hydrogen atoms are more strongly bound in the system. This explains the trend in part (I) of Fig. 6. What is interesting about Fig. 6(a) is the change in the change in the slope of the curve (II) after slightly more than a half the hydrogen atoms have been abstracted from the system. The reason for this change is that metallization dominates over ionization. We can think of this stage as a situation whereby hydrogen atoms are dissolved in Na metal matrix, with the metal retaining its metallic nature. The scattering in Fig. 6(a) is related to the rearrangement and cluster fragmentation during the abstraction process. Figure 6(b) shows the desorption energy as a function of the number of H_2 molecules desorbed. The desorption energy is defined as

$$E^{\text{desorb}} = [E_{\text{Na}_{48}} + E_{n/2\text{H}_2}] - E_{\text{Na}_{48}\text{H}_n}, \tag{3}$$

where $n=2,4,6,8,\ldots,48$.

From Fig. 6(b), one deduces that the desorption energy for $Na_{48}H_{48}$ cluster on average is about 14 kcal/mol Na. This is interesting since it means that the molecular hydrogen desorption energy for a completely dehydrogenated $Na_{48}H_{48}$ cluster is more than the bulk desorption energy (11.6 kcal/mol NaH). One reason for this is the steric interactions arising from the hydrogens in the bulk-phase repulsing each other by means of Coulomb and three-body interactions, so an isolated H atom in a cluster may have a higher abstraction energy.

The charge distribution plots for four different conformations during the abstraction runs is shown in Fig. 7. The hydrogen atoms are negatively charged.

In Fig. 7(a), one observes that the surface sodium atoms, which have a small number of hydrogen atom neighbors, have a small charge. The same applies for hydrogen atoms. As one moves from Fig. 7(a) to Fig. 7(d), the distribution of sodium charges tends toward the lower numbers. This illustrates the decrease in ionicity, which is dependent on the number of neighbors, with increasing abstraction of surface molecular hydrogen. The hydrogen atoms, on the other hand, acquire more neighbors with a concomitant increase in their charges. In Fig. 7(a), we see some hydrogen atoms with a charge of −0.5. These are the surface hydrogen atoms, which have fewer number of neighbors. In Fig. 7(d), the charge distribution on sodium atoms is between 0 and 0.3, implying that the electrons (by inference) are delocalized within the system. Thus, the system gradually loses its ionic character and tends toward metallization.

A. Cluster size dependence effects (nanostructuring)

An obvious choice for increasing the kinetics of hydrogen absorption and desorption is nanostructuring. In the nan-

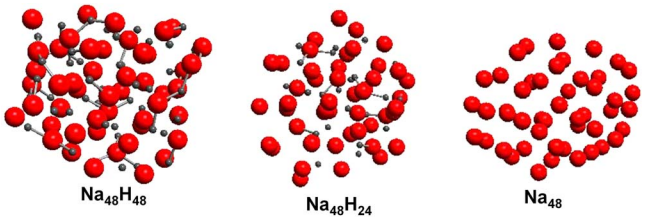

FIG. 5. (Color online) Geometries of the annealed structures of $Na_{48}H_{48}$, $Na_{48}H_{24}$, and Na_{48}. The big balls represent sodium atoms.

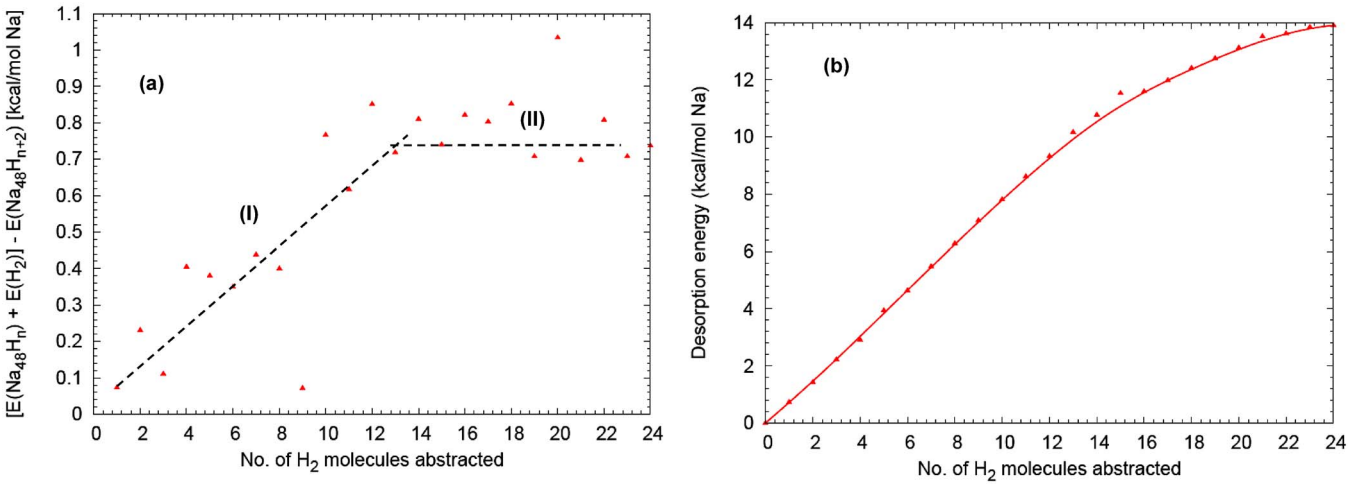

FIG. 6. (Color online) (a) Abstraction energy, $\Delta E=\{[E(\mathrm{Na_{48}H}_n)+E(\mathrm{H_2})]-E(\mathrm{Na_{48}H}_{n+2})\}$. (b) Desorption energy, $E^{\mathrm{desorb}}=[E_{\mathrm{Na_{48}}}+E_{n/2\mathrm{H_2}}]-E_{\mathrm{Na_{48}H}_n}$, as a function of number of H_2 molecules abstracted from the system.

oregime, surface effects dominate over the bulk properties. Nanoclusters also offer a shorter diffusion distances for hydrogen thereby enhancing the diffusion-limited reaction rates. Figure 8 shows the dependance of the total desorption energy on the cluster size. The total desorption energy, which is the energy needed to desorb all the hydrogen atoms from a given cluster, is defined as

$$\Delta H^{\mathrm{des}} = E[n\mathrm{Na}] + \frac{n}{2}E[\mathrm{H_2}] - E[\mathrm{Na}_n\mathrm{H}_n]. \quad (4)$$

Also shown in Fig. 8 are the Na_{400} cluster (about 3.3 nm) and Na_{32} clusters after desorption of all the hydrogen atoms. The figure shows that it easier to desorb all the hydrogen atoms from smaller clusters than from the larger clusters. The total desorption energy converges to a value of 15.5 kcal/NaH for clusters with more than 256 Na atoms. This shows that the NaH having less than 256 Na atoms, which, in turn, relates directly to cluster size, have different behaviors from the bigger clusters. Decreasing cluster size

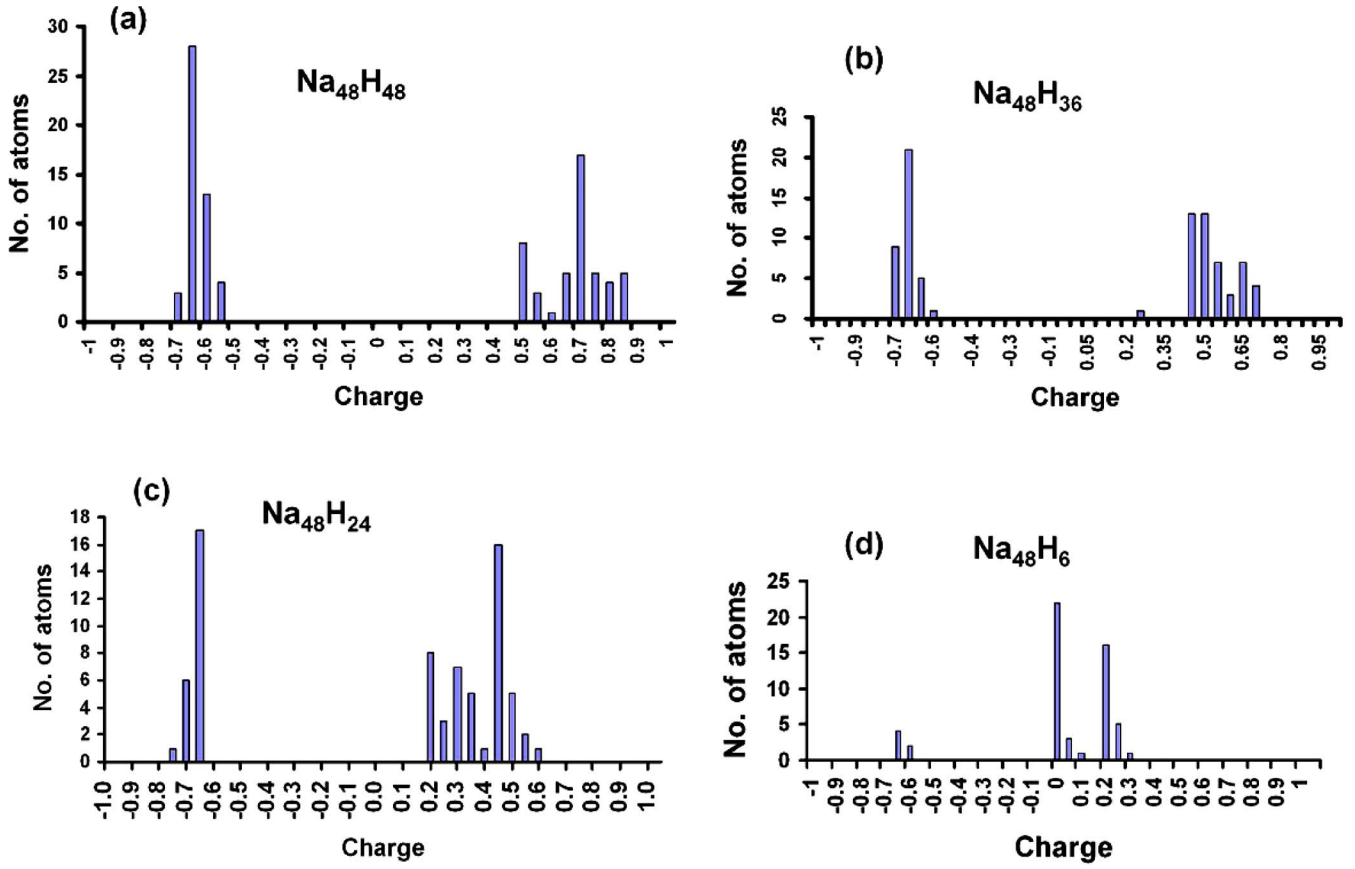

FIG. 7. (Color online) Histograms showing the charge distribution during abstraction of molecular H_2 from $Na_{48}H_{48}$ cluster.

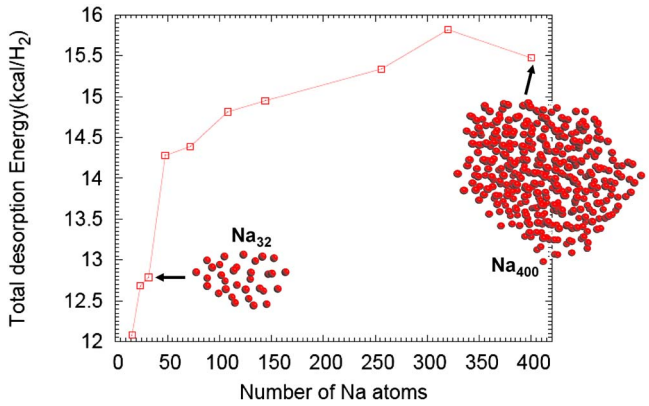

FIG. 8. (Color online) Abstraction energy for all hydrogen atoms from different NaH clusters.

leads to increase in the surface/volume ratio; therefore, for smaller clusters, the average coordination number of surface atoms is reduced, implying a lesser number of bonds. This means that for small clusters, surface effects is dominant and leading to faster kinetics due to weakened bonds. In the case of larger clusters, once the surface molecular hydrogen have been abstracted it becomes increasingly difficult to abstract the remaining hydrogen atoms which are strongly bound within the cluster. This approach makes the fundamental assumption that the cluster does not fragment during the desorption process otherwise the picture becomes quite complicated. There is no experimental evidence to backup our theoretical observations for the nanophase NaH.

IV. MOLECULAR DYNAMICS SIMULATION

$\text{ReaxFF}_{\text{NaH}}$ enables us to investigate the thermally induced desorption of hydrogen molecules in NaH. To do this, we performed a *NVT* simulation on a small NaH cluster ($Na_{48}H_{48}$) by heating it from 100 to 1200 K using Berendsen thermostat.[28] A velocity Verlet algorithm with a time step of 0.25 fs was used in all simulation runs. The heating rate was set at 0.0025 K/ps (2.5×10^9 K/s). The cluster was first minimized to find the nearest metastable state and then equilibrated at 100 K for 5×10^4 steps. The temperature of the system was then increased linearly from 100 to 1200 K as

$$T(t) = T_{100\ \mathrm{K}} + \lambda t, \tag{5}$$

where λ is the heating rate. Figure 9 shows the time evolution of the potential energy (PE) during a heating simulation of NaH from 100 to 1200 K. It can be seen in the figure that at elevated temperatures there are drops in PE, which can be attributed to the decomposition of the cluster and also to the release of molecular hydrogen. Since the heating rate is unphysically fast and temperatures involved are quite high, the heated up cluster fragments into smaller conformations prior to the release of molecular hydrogen. These smaller clusters are stable entities (see Table V). Another reason for drops in PE is that cluster fragmentation and constructive desorption of molecular hydrogen are both associated with bond breaking and bond formation. When a bond breaks, its chemical PE is converted into kinetic energy leading to a temperature

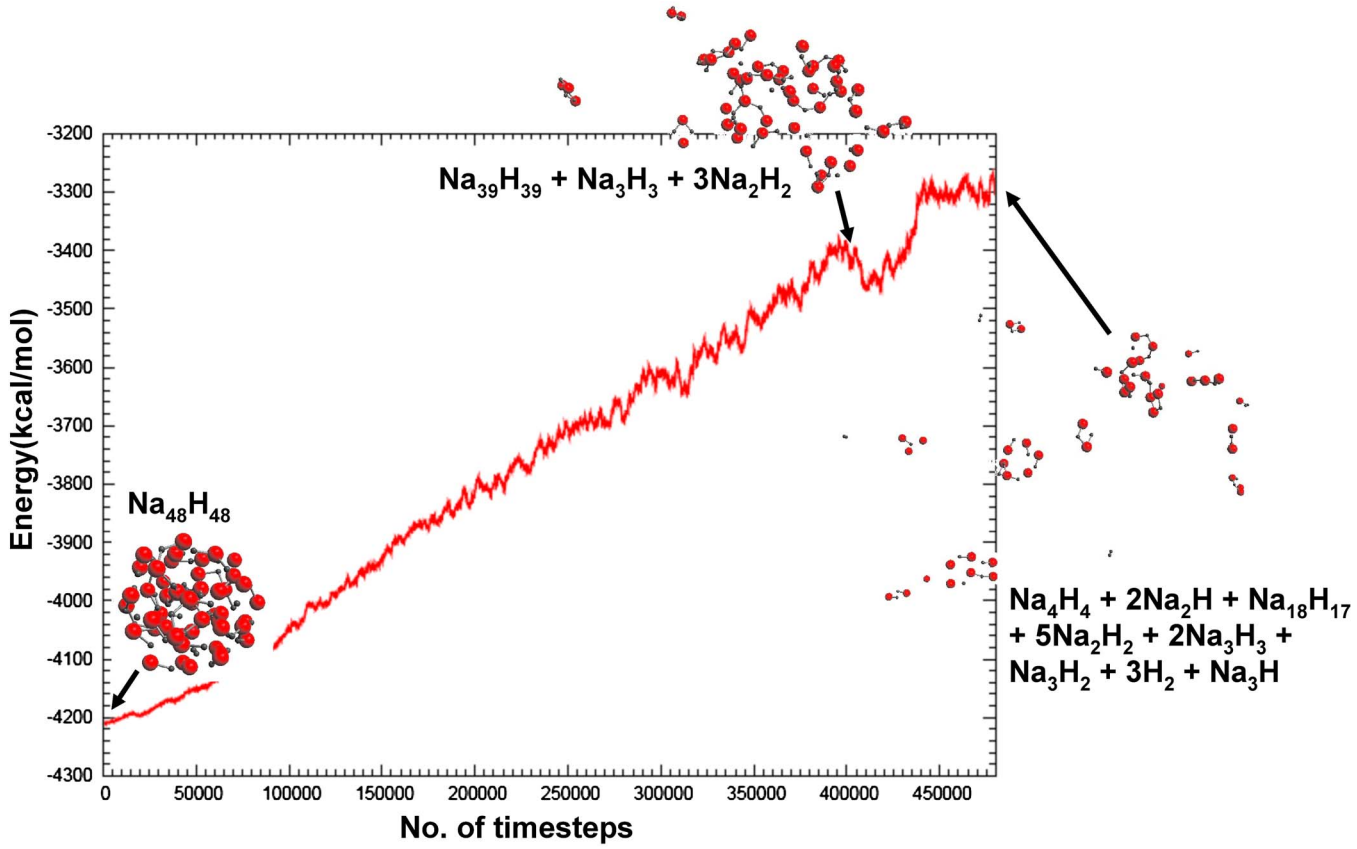

FIG. 9. (Color online) Conformational potential energy landcape during heating of $Na_{48}H_{48}$ cluster from 100 to 1200 K.

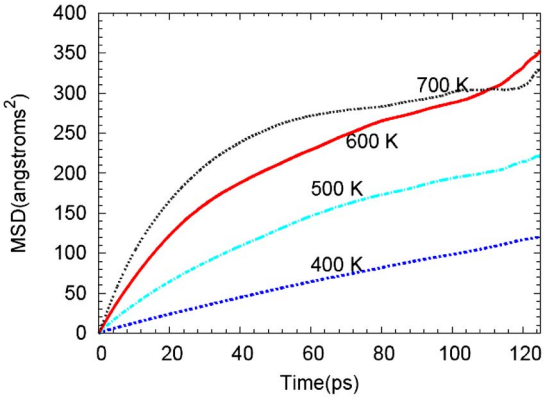

FIG. 10. (Color online) Mean square displacement $\langle \Delta r^2 \rangle$ for different temperatures for hydrogen. The simulation time corresponds to 125 ps, with a time step of 0.25 fs.

rise. This temperature rise results in increased molecular motion whereby the fragmented smaller clusters or the desorbed hydrogen uses this energy to move away from the bigger cluster.

V. DIFFUSION COEFFICIENT OF HYDROGEN

To explore the temperature dependence of diffusion constant of hydrogen atoms on the system, we computed the hydrogen diffusion constant by heating $Na_{320}H_{320}$ at a heating rate of 0.025 K/ps. The system was first heated up to the desired temperature in the range of 300–700 K and then equilibrated for 5×10^4 steps. This was then followed by an averaging run of 5×10^5 steps for each configuration and temperature condition in which diffusional analysis was performed. The diffusion coefficient is calculated from Einstein's relation:

$$D = \lim_{t\to\infty} \frac{\langle [\Delta r^2(t)] \rangle}{6t}, \tag{6}$$

where the mean square displacement (MSD) for each atomic species a is given by

$$\langle \Delta r^2(t) \rangle = \frac{1}{N_a} \sum_i^{N_a} [r_i(t) - r_i(t_0)]^2, \tag{7}$$

with $t=t_0+\Delta t$. The activation energy E_a for diffusion of hydrogen atoms within the cluster can be obtained from Arrhenius law

$$D = D_0 \exp\left(\frac{-E_a}{k_B T}\right). \tag{8}$$

The temperature region considered in this particular computation is 300–700 K since our focus is on the dynamics of the hydrogen atom during the heating process. Below 300 K, there is only thermal vibrations of the atoms and above 750 K there is the possibility of desorption of hydrogen molecule. The MSD for 600 and 700 K deviates from linearity (see Fig. 10). The cause of this deviation is that beyond 600 K, there is partial fragmentation of the cluster into smaller subunits. This adds weight to statistical noise/errors in computation of MSD. If D is to be a constant then a plot of MSD versus time should be linear. For this reason only the linear parts of the MSD plots are considered in the computation of D. The parameters in Eq. (8) can be determined from the temperature dependence of the diffusion constant. Figure 11(a) shows that the diffusion constant rapidly increases with increasing temperature but the trend slightly changes at the 650 K mark due to cluster disintegration. Figure 11(b) shows that the hydrogen atom diffusion constant has an Arrhenius-type temperature dependence for the temperature range considered.

The activation energy for hydrogen diffusion E_a and the pre-exponential factor D_0 were computed using a linear regression analysis of D as a function of $1/T$ [see Eq. (8)]. The calculated pre-exponential is $D_0=3.39\times10^{-3}$ cm^2/s, while the activation energy for hydrogen diffusion in NaH in the temperature range of 350–700 K is 4.1 kcal/mol. The energy cost for diffusion of hydrogen atoms is quite low due to the fact that this is a predominantly an ionic system where electrostatic interactions play a major role. Heating the cluster to elevated temperatures disrupts the ionic lattice, allowing the hydrogen/sodium atoms to easily diffuse within the

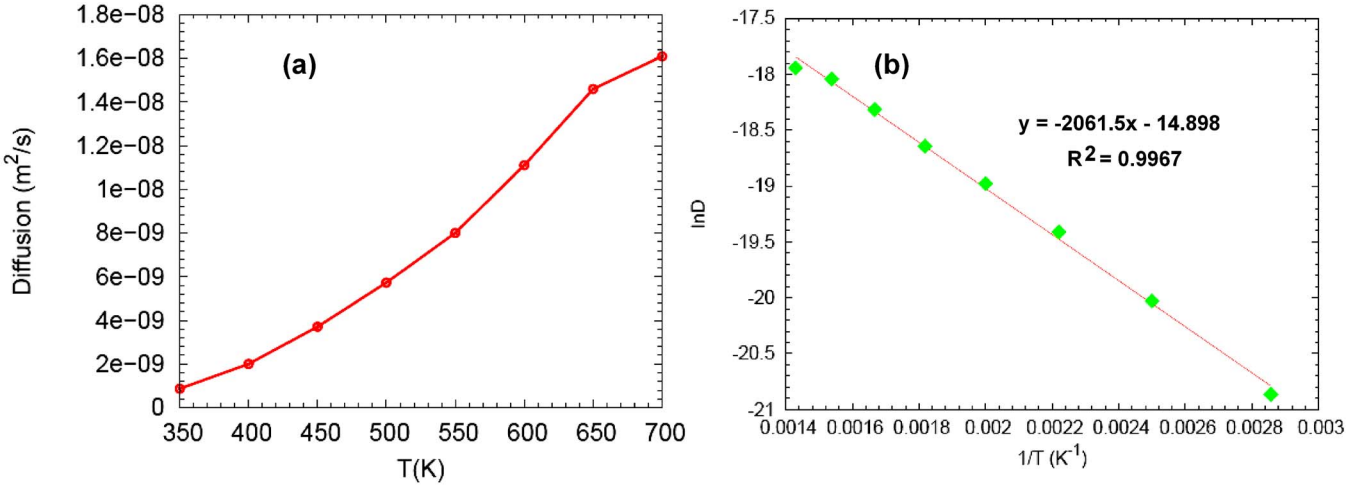

FIG. 11. (Color online) (a) The temperature dependence of diffusion constant and (b) the $1/T$ dependence of $\ln D$.

cluster at low temperatures. The other reason is that the size of our cluster is small and surface effects might play a role in lowering the diffusional energy barrier of hydrogen within the system. It is difficult to apportion the diffusivity of hydrogen atoms in terms of those that diffuse on the surface and those that diffuse within the cluster since in the temperature range considered the highly mobile hydrogen species diffuses randomly within and on the surface of the cluster.

VI. CONCLUSION

A reactive force field ($ReaxFF_{NaH}$) has been parametrized for Na and NaH systems by using DFT derived values for bond dissociation profiles, charge distribution, reaction energy data for small clusters, and equations of state for Na and NaH condensed phases. $ReaxFF_{NaH}$ is built on the same formalism as previous ReaxFF descriptions. We find that $ReaxFF_{NaH}$ correctly reproduces there DFT data. For the atomization of bcc-Na-metal, $ReaxFF_{NaH}$ gives 21.61 kcal/mol, which is consistent with experimental value of 23.28 kcal/mol. DFT and ReaxFF heat of formation studies on NaH clusters both show that as the size of the cluster is increased, its formation energy converges toward the bulk value of −11.60 kcal/mol (ReaxFF) or −10.19 kcal/mol (DFT). ReaxFF also gives bulk modulus of 29.2 GPa, which is comparable to the DFT and experimental values of 23.7 GPa and 19.4 ± 2.0 GPa, respectively.

During molecular dynamics simulations on hydrogen abstractions from NaH cluster run, we observed that charge transfer is correctly described by $ReaxFF_{NaH}$. ReaxFF shows that there is a charge transfer from Na and H atoms and there is a phase transition from metallic hydride to solid solution and finally to metal plus hydrogen molecules. Furthermore, $ReaxFF_{NaH}$ predicts that desorption of hydrogen in smaller clusters is easier than in larger clusters since small particles are easily destabilized due to increase in the surface area versus volume ratio. This indicates that nanostructuring enhances desorption of hydrogen. During a molecular dynamics heating up of NaH cluster, the system was seen to fragment at elevated temperatures which is consistent with experimental evidence indicating that NaH decomposes at the melting point (698 K).[5,29]

ACKNOWLEDGMENTS

This work is part of the research programs of Advanced Chemical Technologies for Sustainability (ACTS), which is funded by Nederlandse Organisatie voor Wetenschappelijk Onderzoek (NWO).

[1] A. Strachan, A. C. van Duin, D. Chakraborty, S. Dasgupta, and W. A. Goddard, Phys. Rev. Lett. **91**, 098301 (2003).
[2] A. C. T. van Duin, A. Strachan, S. Stewman, Q. Zhang, X. Xu, and W. Goddard III, J. Phys. Chem. A **107**, 3803 (2003).
[3] Q. Zhang, T. Çağin, A. C. T. van Duin, W. A. Goddard, Y. Qi, and L. G. Hector, Phys. Rev. B **69**, 045423 (2004).
[4] A. C. T. van Duin, S. Dasgupta, F. Lorant, and W. Goddard III, J. Phys. Chem. A **105**, 9396 (2001).
[5] X. Ke and I. Tanaka, Phys. Rev. B **71**, 024117 (2005).
[6] S. Cheung, W.-Q. Deng, A. C. T. van Duin, and W. Goddard III, J. Phys. Chem. A **109**, 851 (2005).
[7] J. Tersoff, Phys. Rev. Lett. **61**, 2879 (1988).
[8] D. W. Brenner, Phys. Rev. B **42**, 9458 (1990).
[9] M. Z. Bazant and E. Kaxiras, Phys. Rev. Lett. **77**, 4370 (1996).
[10] W. J. Mortier, S. K. Ghosh, and S. J. Shankar, J. Am. Chem. Soc. **120**, 2641 (1998).
[11] G. Kresse and J. Furthmüller, Phys. Rev. B **54**, 11169 (1996).
[12] P. E. Blöchl, Phys. Rev. B **50**, 17953 (1994).
[13] J. P. Perdew, J. A. Chevary, S. H. Vosko, K. A. Jackson, M. R. Pederson, D. J. Singh, and C. Fiolhais, Phys. Rev. B **46**, 6671 (1992).
[14] J. P. Perdew, K. Burke, and Y. Wang, Phys. Rev. B **54**, 16533 (1996).
[15] J. P. Perdew, K. Burke, and M. Ernzerhof, Phys. Rev. Lett. **77**, 3865 (1996).
[16] H. J. Monkhorst and J. D. Pack, Phys. Rev. B **13**, 5188 (1976).
[17] F. Birch, Phys. Rev. **71**, 809 (1947).
[18] R. Dovesi, M. Causa', R. Orlando, C. Roetti, and V. R. Saunders, J. Chem. Phys. **92**, 7402 (1990).
[19] *CRYSTAL2006 User's Manual, University of Torino*, 2006.
[20] G. Gilat and L. J. Raubenheimer, Phys. Rev. **144**, 390 (1966).
[21] Y. Chen, C. H. Huang, and W. Hu, J. Phys. Chem. A **109**, 9627 (2005).
[22] M. W. J. Chase, C. A. Davies, J. R. J. Downey, D. J. Frurip, R. A. McDonald, and A. N. Syverud, J. Phys. Chem. Ref. Data Suppl. **14**, 1 (1985).
[23] M. W. Chase, J. Phys. Chem. Ref. Data Monogr. **9**, 1 (1998).
[24] S. J. Duclos, Y. K. Vohra, A. L. Ruoff, S. Filipek, and B. Baranowski, Phys. Rev. B **36**, 7664 (1987).
[25] B. R. K. Gupta and V. Kumar, Czech. J. Phys., Sect. B **33**, 1011 (1983).
[26] J. L. Martins, Phys. Rev. B **41**, 7883 (1990).
[27] K. Barbalance, http://EnvironmentalChemistry.com/yogi/periodic/Na.html (1995).
[28] H. J. C. Berendsen, J. P. M. Postma, W. F. van Gunsteren, A. Dinola, and J. R. Haak, J. Chem. Phys. **81**, 3684 (1984).
[29] A. F. Hollemann and E. Wiberg, *Lehrbuch der Anorgansichen Chemie* (Walter de Gruyter, Berlin, 1995).
[30] G. D. Barrera, D. Colognesi, P. C. H. Mitchell, and A. J. Ramirez-Cuesta, Chem. Phys. **317**, 119 (2005).